Reaction Monitoring of the MMA Polymerization at Marginal Dispersion Stability

Charalampos A. Mantelis and Thierry Meyer
Ecole Polytechnique Fédérale de Lausanne, Institute of Chemical Sciences and Engineering,
Group of Chemical and Physical Safety, Station 6, CH-1015 Lausanne, Switzerland

DOI 10.1002/aic.11373

The free-radical dispersion polymerization of methyl methacrylate was studied using the reaction calorimetry technique. An especially developed calorimeter for use with supercritical fluids was employed and a set of experiments was explicitly designed to isolate the effect of the pressure. It was found that, under marginal dispersion stability conditions, small pressure changes can have significant effects on the reaction evolution. The pressure was also found to affect the partitioning of the monomer between the two reaction phases. The heat released during the nucleation stage of the reaction was measured for the first time and permitted the discussion on the polymerization locus during this stage. © 2007 American Institute of Chemical Engineers *AIChE J,* 54: 529–536, 2008
Keywords: calorimetry, MMA, monitoring, polymerization, high pressure, $scCO_2$

Introduction

One of the strongly investigated alternatives for solvents in polymerization reactions, during the last two decades is supercritical fluids (SCFs).[1] The main reason is the replacement of tones of hazardous organic and aqueous waste, currently used by the polymer industry as solvents. Among SCFs the most studied is by far supercritical carbon dioxide ($scCO_2$).[2] It has been found to be a very interesting alternative for the development of sustainable chemical process. Its principal advantages are the ability to tune its properties by adjusting the temperature and/or the pressure, its relatively easily attainable critical point ($T_c = 31.1°C$, $P_c = 7.38$ MPa), the fact that it is nontoxic and nonflammable and last but not least its price, being the second cheapest industrial solvent after water. As a result it has been widely employed in various applications, such as the extraction of natural ingredients, mainly for the food and pharmaceutical industry.[3]

Before the 1990's the only example of polymerization in SCFs was the reaction for the production of low density poly (ethylene) (LDPE), where the supercritical component was the solvent and the monomer at the same time. More recently, the ability to use $scCO_2$ as a solvent was examined and the evolution of this technology has been more or less determined by the solvating power of $scCO_2$ for high molecular weight molecules like polymers. The first reactions studied were homogeneous free radical polymerizations for the production of amorphous fluoropolymers and silicones, since these two families of polymers are soluble to $scCO_2$.[4] Later precipitation polymerization systems were developed taking advantage of the fact that the chain transfer to solvent reaction is absent when using $scCO_2$.[5] Finally, three disadvantages of the precipitation polymerization technique, namely low yields, low molecular weight products and the formation of continuous networks instead of regular spherical particles, have led to the development of the main polymerization technique for reaction in $scCO_2$, the dispersion polymerization.[6]

The free-radical dispersion polymerization of methyl methacrylate (MMA) in $scCO_2$ is one of the most studied reactions in this field. An initiator is used to produce, by thermal decomposition, the free radicals which later react with the monomer to produce growing polymer chains. Very rapidly the solubility threshold of the growing oligomers in the supercritical solvent is reached and they phase separate. A surfactant is used to sterically stabilize the precipitating oligomers and form a stable dispersion. The surfactants consist of a CO_2-philic part,

---

Correspondence concerning this article should be addressed to T. Meyer at thierry.meyer@epfl.ch.

usually a fluoropolymer or a silicone, and of a CO_2-phobic part with chemical affinity to the monomer units. As a result the polymerization takes place in two phases, namely the CO_2-rich phase, or continuous phase and the polymer-rich phase.

Several parameters of the above reaction have been previously investigated, such as the stabilizer's type and concentration, the monomer's concentration, and the stirring speed.[7–11] In this work we report the monitoring of the reaction evolution at marginal dispersion stability using the reaction calorimetry method and we investigate the effect of the pressure.

Experimental Part

Materials

MMA (99+% purity, stabilized with ca.0.004% hydroquinone) and 2,2′-azoisobutyronitrile (AIBN) were purchased by Fluka and were used as received. Poly(dimethylsiloxane) monomethacrylate (PDMS-mMA) was purchased by ABCR and had a weight average molecular weight of 5000 g mol^{-1}. Carbon dioxide (quality 30, purity 99.9+%) provided by Carbagaz was used without further purification.

Reaction calorimetry

Reaction calorimetry is a technique amenable to calorimetry which in turn belongs to a greater category of analytical methods, namely the thermal analysis. The objective of reaction calorimetry is to monitor the heat exchange between the contents of a reactor vessel and its surroundings.[12] The heat released or absorbed by a global reaction (exothermic or endothermic respectively) is an unmistakable trace of its evolution, thus the reaction can be closely followed using the reaction calorimetry principal.

$$[\text{Accumulation}] = [\text{Source}] + [\text{Inflow}] - [\text{Outflow}]$$

Further, each term of the above heat balance can be substituted with mathematical terms expressing the corresponding individual heat flow terms as shown in Figure 1:

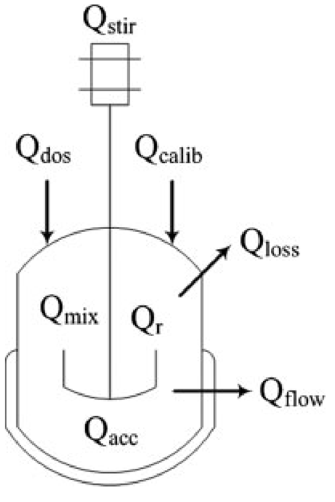

Figure 1. Schematic representation of the heat flow equation.

$$\begin{aligned}&\dot{Q}_{\mathrm{acc}} = \dot{Q}_{\mathrm{r}} + \left(\dot{Q}_{\mathrm{dos}} + \dot{Q}_{\mathrm{mix}} + \dot{Q}_{\mathrm{stir}} + \dot{Q}_{\mathrm{calib}}\right) - \left(\dot{Q}_{\mathrm{flow}} + \dot{Q}_{\mathrm{loss}}\right)\\ &\Rightarrow \dot{Q}_{\mathrm{r}} = \dot{Q}_{\mathrm{flow}} + \dot{Q}_{\mathrm{acc}} - \dot{Q}_{\mathrm{calib}} - \dot{Q}_{\mathrm{stir}} + \dot{Q}_{\mathrm{loss}} - \dot{Q}_{\mathrm{dos}} - \dot{Q}_{\mathrm{mix}}\end{aligned} \tag{1}$$

Once the heat released by the reaction is calculated, the enthalpy of the reaction can be found and consequently the reaction rate and the conversion evolution, according to the following equations.

$$\Delta H_{\mathrm{r}} = \frac{\int_{t_0}^{t_{\mathrm{f}}} \dot{Q}_{\mathrm{r}} dt}{m X_{\mathrm{f}}} \tag{2}$$

$$r = \frac{\dot{Q}_{\mathrm{r}}}{V(-\Delta H_{\mathrm{r}})} \tag{3}$$

$$X(t) = \frac{\Delta H_{\mathrm{r}}(t)}{\Delta H_{\mathrm{r}}} X_{\mathrm{f}} = \frac{\int_{t_0}^{t_{\mathrm{f}}} \dot{Q}_{\mathrm{r}} dt}{\int_{t_0}^{t_{\mathrm{f}}} \dot{Q}_{\mathrm{r}} dt} X_{\mathrm{f}} \tag{4}$$

In the case of reaction calorimetry with SCFs the particularities linked to the supercritical state of the solvent must be taken into consideration. In essence this means that the constant volume specific heat capacity of the reaction mixture must be used for the accumulation term, the heat provided during the injection of additional reactants must be accounted for, and the contribution of the reactor cover and flange in the heat flow term must be included in the calculations.

Experimental set-up

The experimental set-up mainly consists of a high pressure reactor coupled with an RC1*e* reaction calorimeter. The reactor's maximum operating pressure and temperature are 35 MPa and 300°C respectively. It is equipped with a Pt100 temperature sensor, a pressure sensor, a magnetic stirrer connected to a double stage turbine, and a calibration heater. The thermostat unit and two additional controllers create the interface with a personal computer and allow for piloting the entire installation. Furthermore, the calorimeter provides the possibility to work in three different modes; isothermally, isoperibolically and adiabatically. Additional equipment includes a high pressure syringe pump for the addition of reactants and a high precision coriolis mass flow meter coupled to a piston pump for the charging of the reactor with CO_2. A more detailed description and a schematic representation of the experimental set-up can be found elsewhere.[10]

Polymer characterization

The molecular weight distribution (MWD) and the weight average molecular weight of the polymer samples obtained from the experiments in this study were measured using triple detection size exclusion chromatography (Viscotek, SEC^3 TDA300, refractive index, light scattering, and viscometry, solvent THF at 40°C, 1 mL min^{-1} flow rate, ~0.005 g mL^{-1} polymer, 100 μL injection). The device was calibrated using PMMA standards (HR2/3/4). Images of the polymer samples were obtained with scanning electron microscopy (JEOL, XL30 FEG, accelerating voltage 2–3 kV, spot size 2–3 nA). The samples were gold coated to a thickness of ~350 Å. Particle size distribution (PSD) measurements were carried out

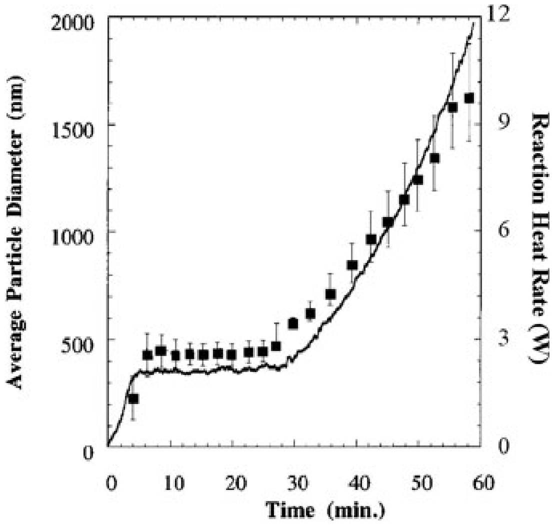

Figure 2. Qualitative comparison of the average particle diameter (filled squares, MMA in $scCO_2$, at 65°C, 5wt % PDMS-mMA/MMA, ~20 wt % MMA/CO_2[16]) and the reaction heat rate evolution (line, MMA in $scCO_2$, at 65°C, 10 wt % PDMS-mMA/MMA, 25wt % MMA/CO_2 [this study]) during the nucleation phase.

using laser diffraction (Malvern Mastersizer S) on a particle volume basis. The samples were dispersed in isopropanol (~350 g PMMA in ~50 mL isopropanol), treated for 5 min in an ultrasonic bath (Telsonic, TUC150m 150W/41) and magnetically stirred for another 10 min prior to the measurements.

Polymerization reaction

To perform correct calorimetric calculations and obtain reliable results it is imperative that the reaction temperature is attained before the reaction begins; therefore one of the reactants was kept separately until the temperature was set. The reactor was first charged with part of the monomer and the desired amount of stabilizer. It was sealed, purged intensively with CO_2 to eliminate any trace of oxygen and charged with the desired amount of CO_2. Then it was heated to the reaction temperature and finally a mixture of the rest of the monomer and the initiator was injected in the reactor. The initiator being solid had to be dissolved in monomer to produce a homogeneous liquid mixture that could be injected through the syringe pump. A series of solubility measurements has shown that a minimum of 12 ml of MMA per gram of AIBN are necessary to obtain easily a homogeneous mixture at ambient temperature. From the point of injection it was considered that the reaction was launched and the calorimetric calculations commenced.

A set of conditions was chosen for the free-radical polymerization reaction as a base case scenario and served as the point of reference.

- Reaction temperature: 80°C.
- Reaction pressure range: 21.3–24.4 MPa.
- Initial MMA mass in reactor: 224.41 g.
- Stabilizer used: Poly(dimethylsiloxane) monomethacrylate (PDMS-mMA).
- Stabilizer mass: 25.28 g (10 wt % PDMS-mMA/MMA).
- Injection solution composition: 2.528 g AIBN/28.61 g MMA (1 wt % AIBN/MMA).
- Solution injection method: constant flow at 5 mL min^{-1}.
- CO_2 mass: 680 g.
- Stirring speed: 400 rpm.

Under the above conditions the initial reaction mixture was optically observed to be homogeneous and transparent. Such observation was expected since Fortini has previously found the cloud point pressure of a 30 wt % MMA/CO_2 and 13 wt % PDMS-mMA/MMA mixture at 80°C to be 12.3 MPa.[13] In our case the higher MMA/CO_2 ratio is bound to decrease even further the cloud point pressure due to the cosolvent effect; therefore the initial pressure positions the reaction mixture well within the homogeneous region. However very shortly after the launch of the reaction the first polymer particles are formed and the reaction mixture becomes opaque.

Although most of the past research on the free-radical dispersion polymerization of MMA in $scCO_2$ has been conducted at 65°C, the choice of 80°C in our investigations was necessary. The reason lies on the necessity for the calorimetric calculations of a reaction system that can be thermally homogeneous throughout the entire reaction. Only then the calorimeter can maintain the reactor temperature steady for the execution of isothermal experiments. At 65°C the balance is delicate between high reactants' concentrations to achieve adequate pressures for the dispersion formation but which result in temperature inhomogeneities in the reactor, and low reactants' concentrations to avoid the latter but that result in insufficient pressures so that the stabilizer macromolecules can be dissolved and the dispersion formed. As a result at 65°C a thorough and complete investigation of the polymerization using the reaction calorimetry technique is not feasible.

Results and Discussion

Particle formation stage of the polymerization reaction

The polymer particles' formation mechanism during the early stage of the reaction was first reported by Paine for dispersion polymerizations in liquid media.[14] For the case of MMA in $scCO_2$ an analogous, but more complex, mechanism was later proposed based on turbidimetry measurements and states that as polymer chains grow above a critical length they are no longer soluble to the CO_2-rich phase and they phase

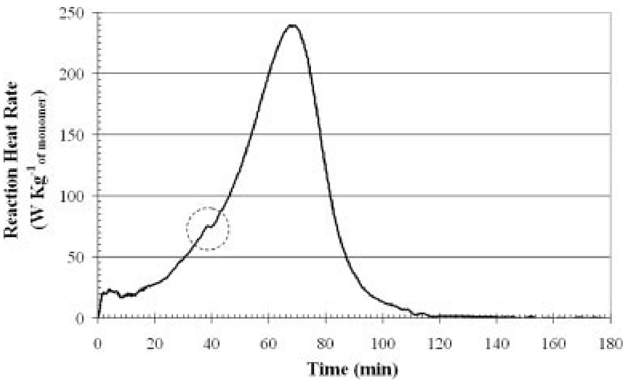

Figure 3. Reaction deceleration observation at the base case conditions.

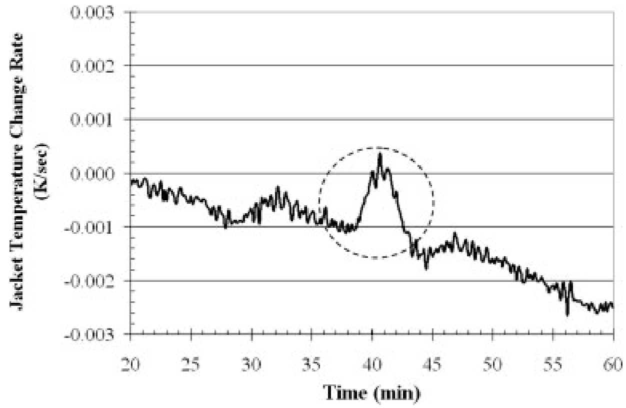

Figure 4. Jacket temperature change rate during the reaction deceleration.

separate.[15–17] This threshold value is apparently very low, since even oligomers of 30 repeated units are completely insoluble in pure $scCO_2$ at 20 MPa and 35°C.[18] Once the oligomers precipitate, the surfactant stabilization mechanism intervenes and stabilizes the polymer particles forming the dispersion. During this particle formation two distinct phases have been identified, namely the coagulative nucleation and the controlled coagulation.[19]

Using the supercritical reaction calorimetry technique we have been able to monitor for the first time the heat released by the reaction during the above phases and comment on the overall reaction rate. A direct qualitative comparison demonstrates a similarity between the evolution of the average particle diameter as reported by O'Neill et al. and the evolution of the overall heat released by the reaction (Figure 2).[6] During the coagulative nucleation phase the period of constant particle size indicates that the main locus of polymerization is the continuous phase. This estimation is now also supported by the calorimetric results that show an almost constant reaction heat rate, which in turn reveals a constant overall reaction rate. This reaction rate is characteristic of an environment with no restrictions on the mass transfer of the growing polymer chains and no effect of the monomer consumption, such as the continuous phase at the very early stages of the reaction where the overall conversion is less than 1%. On the other hand, when the reaction moves to the controlled coagulation phase, the reaction heat rate increases revealing a reaction acceleration. The latter is characteristic of the Trommsdorff effect indicating that the reaction is now taking place also inside the polymer particles. This observation is also supported by the increasing polymer particles' size.

The slightly higher MMA/CO_2 ratio of approximately +5 wt % used in the reaction heat rate monitoring experiment, although it is expected to produce more favorable conditions in terms of dispersion stability, through a more pronounced cosolvent effect, it is not expected to affect our qualitative conclusions on the reaction evolution during the particle formation stage, especially since the initial reaction pressures are almost identical and equal to 20.5 MPa. Furthermore, the difference between 5 and 10 wt % in the PDMS-mMA/MMA ratio has been found in a previous study not to affect the reaction evolution as well as the characteristics of the final polymer product.[10]

Reaction deceleration at marginal dispersion stability

The experimental results of the reaction heat rate at the base case polymerization conditions are presented in Figure 3 and they demonstrate a small reaction deceleration after approximately 40 min from the reaction launch, where the reaction for a very short period of time evolves at a constant rate. To illustrate better this observation the jacket temperature change rate is plotted with time in Figure 4, where it is shown that the jacket temperature during this period remains stable; meaning that the heat released by the reaction is stable too.

For the design of an appropriate set of experiments in order to investigate this observation, it was taken into account that previous tests on the same polymerization system but at higher pressure, due to higher CO_2 mass, do not demonstrate this deceleration.[13] Additionally, previous reports on the effect of different ratios between the monomer, the solvent and the stabilizer quantities also do not show such a deceleration, because the initial reaction pressure is always higher.[10] Therefore, it was reasonable to conclude that the appearance of this step in the reaction rate was related to the lower pressure. Furthermore, since all of the experiments were conducted in the same isochoric system, the origin of the deceleration was linked to the concentrations of the reactants that define the system's pressure. However, in order to investigate only the effect of the pressure the ratios of the reactants were kept constant and equal to the base case and only their absolute quantities were varied at specific percentages with respect to the base case, as shown in Table 1. As a result the reaction evolution was monitored in different pressure regimes.

As far as the lower pressure, or else lower concentration, experiments are concerned, Figure 5 shows that the jacket temperature decreases much more slowly, indicating that the reaction rate is much lower. In the case of −1%, the final product instead of a white fine powder was a sticky dense white liquid, indicating a very poor dispersion formation. The latter resulted in nonhomogeneous concentration and temperature conditions in the reactor that led to the observed loss of temperature control. The combination of the slower reaction rate shown in Figure 6 and the larger heavily agglomerated polymer particles formed in the −0.5% case, as demonstrated by the SEM pictures in Figure 7, indicate that less polymer particles are actually stabilized by the stabilizer. As a result the acceleration

Table 1. Masses of All Reactants in the Pressure Investigation Set of Experiments and the Respective Initial Pressures

	−1%	−0.5%	Base Case	+1%	+2%	+3%	+7%
Monomer mass (g)	250.27	251.54	252.80	255.33	257.86	260.38	270.50
CO_2 mass (g)	673.00	677.00	680.00	687.00	694.00	701.00	728.00
Stabilizer mass (g)	25.03	25.15	25.28	25.53	25.79	26.04	27.05
Initiator mass (g)	2.50	2.52	2.53	2.55	2.58	2.60	2.71
Initial pressure (mPa)	19.5	19.7	21.3	22.4	23.8	24.4	28.8

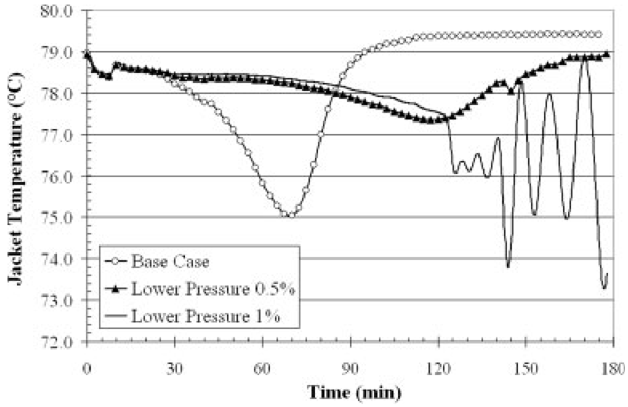

Figure 5. Comparison of the jacket temperature variation between the base case and the lower pressure experiments.

of the reaction rate due to the Trommsdorff effect is smaller and the observed reaction rate step is more pronounced. Overall it is found that the base case conditions are close to the limit of the dispersion formation and a very small decrease in the concentrations and hence the initial pressure has a dramatic effect on the dispersion formation and eventually on the reaction evolution.

On the other hand for slightly higher reaction pressure (+1%), the jacket temperature change rate evolution shows that the reaction deceleration moves forward in time and for even higher pressures (+2% and higher) it completely disappears (Figure 8). Furthermore, the reaction heat rate, during the particle formation stage, was found to be higher and the consequent reaction acceleration was found to start earlier (Figure 9).

Identifying the expected effects of the reactants' higher concentrations helps justify the above observation. Firstly, the increased concentration of the initiator results in the production of more free radicals. However, the resulting higher pressure, from 21.3 to 28.8 MPa, is found by calculations on the decomposition of AIBN to have a negligible effect on its rate coefficient (k_d) as well as on its efficiency (f).[20] Secondly, the higher stabilizer concentration is expected to facilitate the formation of the polymer particles. Thirdly, the MMA and CO_2 higher concentrations, which are the two principal components of the continuous phase, increase this phase's density and thus its solvation power for the stabilizer macromolecules; therefore a better dispersion formation is expected. Finally the resulting higher pressure induces a more favorable partitioning of the monomer in the CO_2-rich phase according to Lora et al., which have previously reported that at higher pressures CO_2 and MMA mix better.[21]

As far as the continuous phase is concerned the effects of the increased reactants' concentrations and of the more favorable partitioning of MMA explain the higher reaction rate observed in Figure 9. The former also indicate that a larger in volume polymer-rich phase is formed at higher pressures, which is attributed not to the formation of a larger number of particles but to the formation of bigger in size initial polymer particles. This is based on the results of O'Neill et al. on the particle number density, which was found to remain constant for pressures above 20 MPa during the coagulative nucleation phase.[16] Consequently the interfacial area of the dispersed phase increases and this indicates a more rapid shift of the polymerization locus in the polymer-rich phase. Hence the

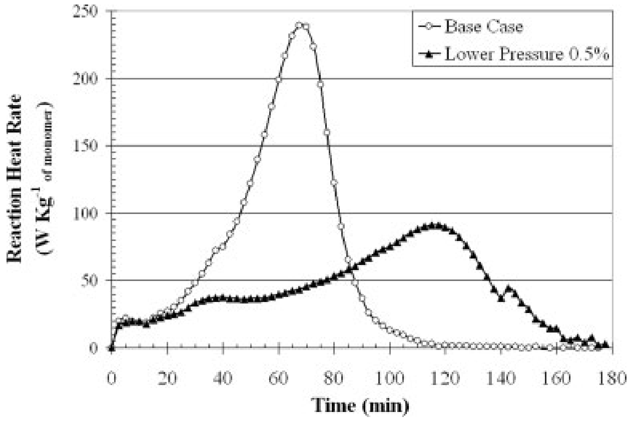

Figure 6. Comparison of the reaction heat rate per kilogram of monomer between the base case and the 0.5% lower pressure experiment.

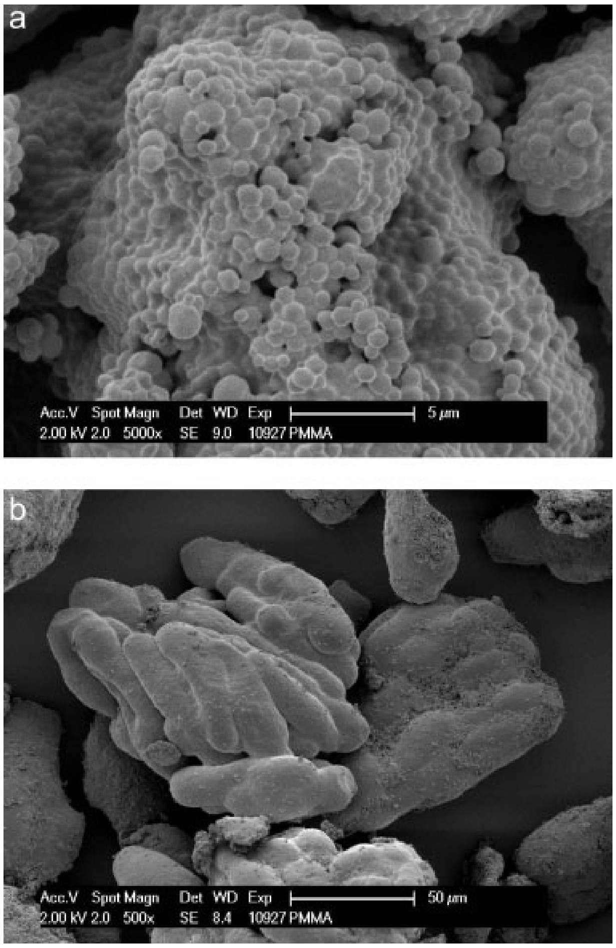

Figure 7. SEM pictures of the base case polymer sample (a) and the −0.5% case (b).

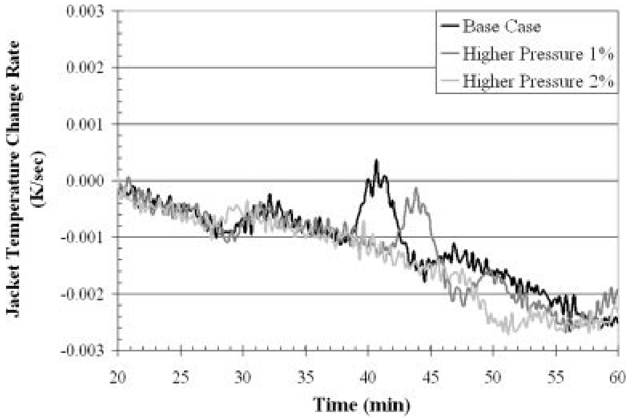

Figure 8. Comparison of the jacket temperature change rate between the base case and the higher pressure experiments.

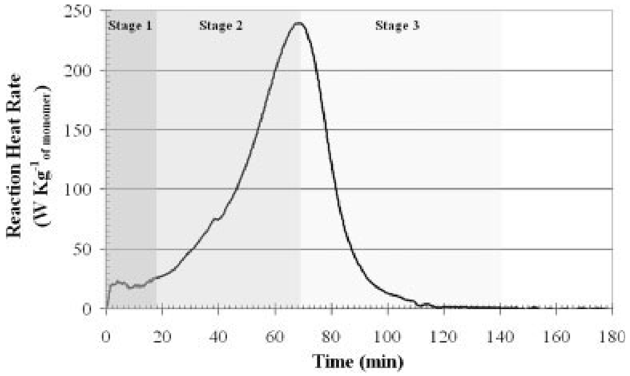

Figure 10. Identification of three stages during the polymerization reaction, based on the reaction rate evolution at the CO_2-rich phase and the polymer-rich phase.

reaction acceleration due to the Trommsdorf effect starts earlier as presented also in Figure 9.

Finally, the disappearance of the reaction deceleration step, shown in Figure 8, can be justified based on the above arguments and the following considerations on the evolution of the reaction rates in each of the three stages, as presented in Figure 10. The expected evolution for the part of the reaction that takes place in the CO_2-rich phase is an almost constant reaction rate during the coagulative nucleation phase (Stage 1). However, as the monomer is consumed from the reaction and also diffused in the polymer particles, its concentration will decrease significantly and the reaction rate is expected to eventually decrease (Stage 2 or 3). As far as the polymer-rich phase part of the reaction is concerned, its contribution to the overall reaction rate is initially negligible (Stage 1). Later, as the polymer particles grow, its contribution becomes predominant leading to the observed reaction acceleration (Stage 2). Eventually the monomer in the particles is also consumed and the reaction rate in that phase reduces too (Stage 3).

Hence, at lower pressure regimes, where the dispersion formation conditions are less favorable and the reactants concentrations smaller, the decrease in the reaction rate of the CO_2-rich phase occurs during Stage 2 and the overall reaction rate observed demonstrates a step. On the other hand, at higher pressures the decrease in the CO_2-rich phase reaction rate occurs much later during Stage 3 and therefore it cannot be distinguished from the more significant reaction rate decrease in the polymer-rich phase.

The argument that the reaction in the CO_2-rich phase, as the pressure increases, continuous steadily for a longer period of time is also supported by the MWD analysis of the samples (Figure 11). The MWD of the lower pressure sample, because of the nonsufficient stabilization of the particles, shows an additional shoulder at ~2600g mol^{-1}, which is the polymer produced in the continuous phase. As the pressure increases the MWD of the base case becomes monomodal with its peak at ~100,000 g mol^{-1}, since the primary locus of the polymerization is the polymer particles. However, the longer tail of the distribution towards lower molecular weights remains, because the reaction in the continuous phase never fully ceases. Increasing the pressure even more, results in the reappearance of the second shoulder in the MWDs (+2% and +3% samples). This time the additional polymer produced in the continuous phase is not the result of an inefficient stabilization of the particles but the result of the enhanced reaction in the CO_2-rich phase.

Finally, as far as the polymer particles formed are concerned, PSD analysis in Figure 12 shows that once the stable dispersion conditions are well established and no deceleration

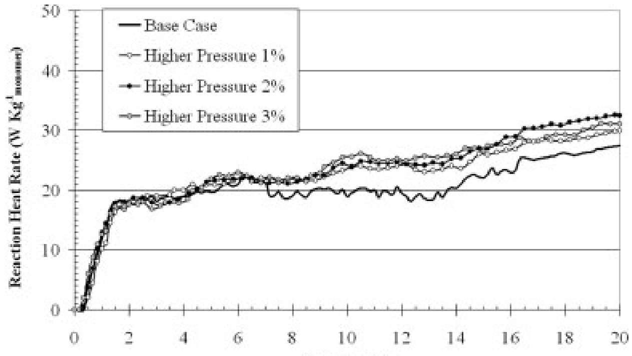

Figure 9. Reaction heat rate during the particle formation stage at higher pressure experiments.

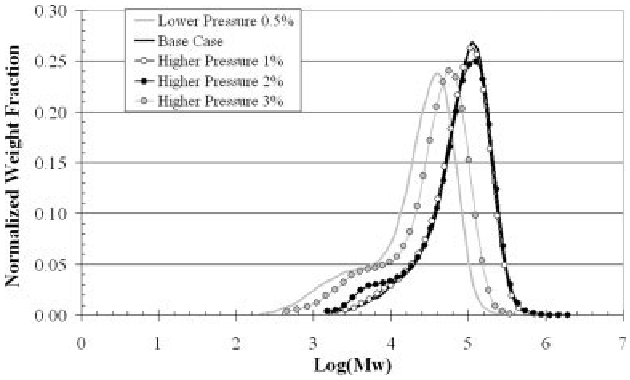

Figure 11. MWD analysis of the polymer samples of the different pressure experiments.

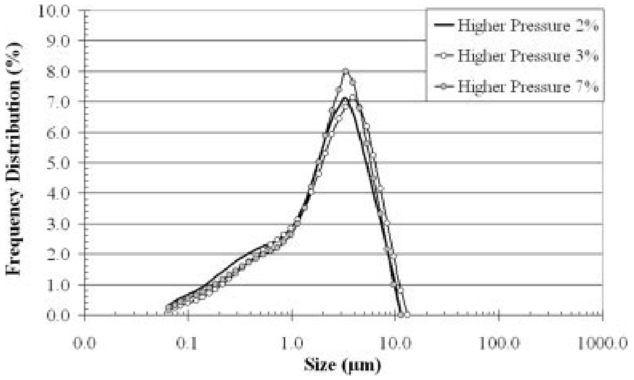

Figure 12. Particle size distribution analysis of the polymer samples obtained at higher reaction pressures.

is observed the polymer particles formed have the same size distribution.

Conclusions

The reaction calorimetry technique was employed to study the reaction evolution of the free-radical dispersion polymerization of MMA in $scCO_2$. The rate with which heat was released from the model reaction was used to monitor the overall reaction rate, especially during the coagulative nucleation phase. The results agree with previously reported observations from other monitoring techniques on that the main locus of polymerization during the particle formation stage is the continuous phase.

The conditions chosen as the base case scenario were found to be under marginal dispersion stability and a set of experiments revealed the role of the pressure in the reaction evolution. The pressure in the isochoric reactor is directly linked to the reactants' concentrations and was found to affect the partitioning of the monomer between the two reaction phases and the solubility of the stabilizer in the continuous phase. As a result at higher pressures the reaction rate in the continuous phase was found to decrease much later.

Supercritical reaction calorimetry is shown to be an accurate and useful tool for the monitoring of reactions with SCFs because it provides important information about the kinetics of the reacting system. The experimental data can be furthermore used to perform thermal safety analysis studies.

Acknowledgments

The Swiss National Science Foundation is gratefully acknowledged for its financial support through the project 200020-109051. The Interdisciplinary Center for Electron Microscopy (CIME) is acknowledged for the help on the SEM analysis of the samples, as well as the Powder Technology Laboratory (LTP) for the PSD analysis.

Notation

AIBN = 2,2′-azoisobutyronitrile
LDPE = low density poly(ethylene)
M = mole of monomer (mol)
MMA = methyl methacrylate
MWD = molecular weight distribution
P = pressure (MPa)
P_c = critical pressure (MPa)
PDMS-mMA = poly(dimethylsiloxane) monomethacrylate
PMMA = poly(methyl methacrylate)
PSD = particle size distribution
$\dot{Q}_r$ = rate with which heat is generated by the reaction (W)
$\dot{Q}_{flow}$ = rate with which heat flows from the reactor to the jacket (W)
$\dot{Q}_{acc}$ = rate with which heat accumulates in the reactor (W)
$\dot{Q}_{calib}$ = rate with which heat is generated by the calibration heater in the reactor (W)
$\dot{Q}_{stir}$ = rate with which heat is generated by the stirrer in the reactor (W)
$\dot{Q}_{loss}$ = rate with which heat is lost either by the reactor, the jacket or the surrounding devices due to secondary reasons (e.g. radiation) (W)
$\dot{Q}_{dos}$ = rate with which heat is inserted in the reactor by the dosing of the reactants (W)
$\dot{Q}_{mix}$ = rate with which heat is generated due to mixing (W)
R = reaction rate (mol s^{-1} m^{-3})
$scCO_2$ = supercritical carbon dioxide
SCF = supercritical fluid
SEM = scanning electron microscopy
T_c = critical temperature (°C)
THF = tetrahydrofuran
T_0 = time zero, before the reaction start (sec)
t_f = time at the end of the reaction (sec)
V = reactor volume (m^3)
X_f = final monomer conversion
ΔH_r = enthalpy of reaction (KJ mol^{-1})

Literature Cited

1. Kendall JL, Canelas DA, Young JL, DeSimone JM. Polymerizations in supercritical carbon dioxide. *Chem Rev*. 1999;99:543–563.
2. Kemmere M, Meyer T, editor. *Supercritical Carbon Dioxide in Polymer Reaction Engineering*. Weinheim: Wiley-VCH, 2005.
3. Perrut M. Supercritical fluid applications: industrial developments and economic issues. *Ind Eng Chem Res*. 2000;39:4531–4535.
4. Desimone JM, Guan Z, Elsbernd CS. Synthesis of fluoropolymers in supercritical carbon-dioxide. *Science*. 1992;257:945–947.
5. Romack TJ, Desimone JM, Treat TA. Synthesis of teatrafluoroethylene-based, nonaqueous fluoropolymers in supercritical carbon-dioxide. *Macromolecules*. 1995;28:8429–8431.
6. Desimone JM, Maury EE, Menceloglu YZ, McClain JB, Romack TJ, Combes JR. Dispersion polymerizations in supercritical carbon-dioxide. *Science*. 1994;265:356–359.
7. Christian P, Giles MR, Griffiths RMT, Irvine DJ, Major RC, Howdle SM. Free radical polymerization of methyl methacrylate in supercritical carbon dioxide using a pseudo-graft stabilizer: effect of monomer, initiator, and stabilizer concentrations. *Macromolecules*. 2000;33: 9222–9227.
8. Giles MR, Hay JN, Howdle SM, Winder RJ. Macromonomer surfactants for the polymerisation of methyl methacrylate in supercritical CO_2. *Polymer*. 2000;41:6715–6721.
9. Giles MR, O'Connor SJ, Hay JN, Winder RJ, Howdle SM. Novel graft stabilizers for the free radical polymerization of methyl methacrylate in supercritical carbon dioxide. *Macromolecules*. 2000;33: 1996–1999.
10. Mantelis CA, Barbey R, Fortini S, Meyer T. Free-radical dispersion polymerization of methyl methacrylate in supercritical carbon dioxide: a parametric analysis with reaction calorimetry. *Macromol React Eng*. 2007;1:78–85.
11. Rosell A, Storti G, Morbidelli M, Bratton D, Howdle SM. Dispersion polymerization of methyl methacrylate in supercritical carbon dioxide using a pseudo-graft stabilizer: role of reactor mixing. *Macromolecules*. 2004;37:2996–3004.
12. Regenass W. The development of heat flow calorimetry as a tool for process optimization and process safety. *J Therm Anal*. 1997;49:1661–1675.
13. Fortini S. Reaction calorimetry in supercritical fluids: a study of the dispersion polymerization of methyl methacrylate in supercritical carbon dioxide. PhD Thesis, Ecole Polytechnique Fédéral de Lausanne, 2005.

14. Paine AJ. Dispersion polymerization of styrene in polar-solvents 7. A simple mechanistic model to predict particle-size. *Macromolecules.* 1990;23:3109–3117.
15. Fehrenbacher U, Ballauff M. Kinetics of the early stage of dispersion polymerization in supercritical CO_2 as monitored by turbidimetry. II. Particle formation and locus of polymerization. *Macromolecules.* 2002;35:3653–3661.
16. O'Neill ML, Yates MZ, Johnston KP, Smith CD, Wilkinson SP. Dispersion polymerization in supercritical CO2 with siloxane-based macromonomer. II. The particle formation regime. *Macromolecules.* 1998;31:2848–2856.
17. O'Neill ML, Yates MZ, Johnston KP, Smith CD, Wilkinson SP. Dispersion polymerization in supercritical CO_2 with a siloxane-based macromonomer. I. The particle growth regime. *Macromolecules.* 1998;31:2838–2847.
18. O'Neill ML, Cao Q, Fang R, Johnston KP, Wilkinson SP, Smith CD, Kerschner JL, Jureller SH. Solubility of homopolymers and copolymers in carbon dioxide. *Ind Eng Chem Res.* 1998;37:3067–3079.
19. Li G, Yates MZ, Johnston KP, Howdle SM. In-situ investigation on the mechanism of dispersion polymerization in supercritical carbon dioxide. *Macromolecules.* 2000;33:4008–4014.
20. Guan ZB, Combes JR, Menceloglu YZ, Desimone JM. Homogeneous free-radical polymerizations in supercritical carbon-dioxide. II. Thermal-decomposition of 2,2′-azobis(Isobutyronitrile). *Macromolecules.* 1993;26:2663–2669.
21. Lora M, McHugh MA. Phase behavior and modeling of the poly (methyl methacrylate)-CO_2-methyl methacrylate system. *Fluid Phase Equili.* 1999;157:285–297.

Manuscript received Mar. 20, 2007, and revision received Oct. 16, 2007.